PCCP
Physical Chemistry Chemical Physics

Accepted Manuscript

This article can be cited before page numbers have been issued, to do this please use: R. Zheng, S. Mohammed, Y. Jia, R. HAZRA and G. Gadikota, *Phys. Chem. Chem. Phys.*, 2024, DOI: 10.1039/D4CP04820B.

ROYAL SOCIETY OF CHEMISTRY

rsc.li/pccp

View Article Online
DOI: 10.1039/D4CP04820B

The Effect of H_2 Occupancy Modes in Small and Large Cages of H_2-Tetrahydrofuran Hydrates on the Hydrates Stability and H_2 Storage Capacity

Ruyi Zheng [1, 2], Sohaib Mohammed [1], Yang Jia [1], Rituparna Hazra [1] and Greeshma Gadikota[1,*]

[1] School of Civil and Environmental Engineering, Cornell University, Ithaca, NY 14853

[2] Frontier Institute of Science and Technology, Xi'an Jiaotong University, Xi'an, Shaanxi 710054, China

*Corresponding author: Greeshma Gadikota, email: gg464@cornell.edu

View Article Online
DOI: 10.1039/D4CP04820B

Abstract

Hydrogen storage as hydrates is considered as one of the most environmentally benign approaches to store hydrogen as it requires only water and traces of promoters. However, advancing scalable controls on hydrogen hydrates formation is hindered by the limited understanding of the structure, dynamics and energetics of hydrogen and promoters in the hydrate cages. In this study, molecular dynamic simulation configurations with different occupancy modes of H_2 and Tetrahydrofuran (THF) in the hydrate cages are investigated under the following scenarios: *i*) two H_2 molecules occupying the small cages, *ii*) occupancy of H_2 molecules in the THF-free large cages, and *iii*) co-occupancy of H_2 and THF in one large cage. Exploring these scenarios reveals the impact of occupancy modes on the dynamic motion of guest and water molecules and on the hydrate structure stability. The results show that the occupancy of two H_2 molecules in the small cages reduced the stability of hydrate structure, triggered the inter-cage hopping of H_2 molecules through pentagonal faces, and increased the probability of hydrogen bond formation between THF and cage H_2O molecules. The thermodynamic stability of hydrate cages is increased when the THF-free large cages are occupied by H_2 molecules and the tetrahedral feature of H_2 distribution in the large cages is enhanced when the number of H_2 in one cage increased from two to three. When the large cages are co-occupied by H_2 and THF, the inter-cage migration of H_2 originated from large cages demonstrated two different features, i.e., ballistic motion (MSD $\propto t^2$) due to the tunneling migration behavior in the initial stage and diffusive motion in the late stage. The ballistic migration of H_2 molecules is more favorable for achieving a higher storage capacity. The decay rate of THF orientation is reduced when the interaction between THF and H_2O molecules is stronger. The insights provided by this study are crucial to advance the understanding of hydrogen storages as hydrates for a sustainable energy future.

View Article Online
DOI: 10.1039/D4CP04820B

Keywords: H_2-THF hydrates; Storage capacity; Cage occupancy; Inter-cage migration; Ballistic motion

1. Introduction

Hydrogen (H_2) is a promising energy carrier with a high energy density (~142 MJ/kg), making it an essential vector in the integrated energy system, such as balancing the seasonal fluctuation of energy demand and supply. However, safe and efficient H_2 storage is challenged by its high flammability, low density, and small molecular size. Numerous approaches have been proposed for hydrogen storage, e.g., geological storage, high-pressure-tank storage, and hydrogen storage materials including hydrate-based storage.(1–7) Hydrate-based H_2 storage is a less explored but transformative approach owing to: (i) the ease of recovering the stored H_2 with high purities, (ii) the formation of hydrates at mild pressure and temperature, (iii) environmentally benign features of hydrates compared to other H_2 storage materials, and (iv) stable trapping of H_2 molecules in the hydrate cages, which reduces the risk of H_2 leakage.

Clathrate hydrates are ice-like crystalline solids formed by guest molecules and cages of H_2O molecules that are connected through hydrogen bonds and in which the guest molecules are trapped. Depending on the guest species and thermodynamic conditions, various structures of clathrate hydrates might be formed.(8) In this context, sII structure has been extensively detected in H_2-containing hydrates.(9,10) A unit cell of sII hydrate is composed of 16 small cage and 8 large cages, as shown in **Figure 1**. Each small cage is made of 12 pentagonal faces and each large cage consists of 12 pentagonal and 4 hexagonal faces. The radius of the small and large cages is 3.91 and 4.73 Å respectively, which results in an average lattice parameter of a sII unit cell around 17.31 Å. Both the large and small hydrate cages can accommodate multiple H_2 molecules, which

View Article Online
DOI: 10.1039/D4CP04820B

makes it conducive for storing H_2 in the hydrate form. It has been reported that H_2 storage capacity of 5.3 wt% is achieved for the H_2 hydrates formed in pure water.(11)

The formation of pure H_2 hydrates requires high pressure and low temperature conditions. For instance, the temperature of 140 K is required to form H_2 hydrates at the ambient pressure, while 300 MPa is needed to form pure H_2 hydrates at 280 K(7,11) (see **Figure 1**). Therefore, it is essential to enable H_2 hydrate formation at moderate conditions to make this approach economically viable. Thermodynamic promoters have been considered to enhance the formation of H_2 hydrates under mild conditions as they increase the stability of hydrate structure by occupying the large cages.(12–14) As indicated in **Figure 1**, the addition of THF to H_2 hydrates could reduce the hydrate formation pressure from 300 MPa to 5 MPa at a temperature around 280 K.(9) The presence of thermodynamic promoters greatly improves the economic viability of the hydrate-based H_2 storage approach, however, at the cost of reduced storage capacity. Some representative findings about the storage capacity of H_2 in pure H_2 hydrates and binary H_2-THF hydrates can be found in **Table S1** in *Supplementary Information*. Generally, the storage capacity is higher when more H_2 molecules can be stably accommodated in the small and large hydrate cages. However, the conclusions on the occupancy modes of H_2 in the small and large cages (e.g., single or multiple H_2 occupying one hydrate cage) demonstrate great discrepancy, especially for the binary H_2-THF hydrates. Some researchers suggested that high storage capacity of H_2 is achievable in the H_2-THF hydrates because small cages could accommodate two H_2 molecules or that multiple H_2 molecules might occupy the large cages in the presence or absence of promoters. For instance, Lee and co - workers inferred from NMR results that the small cages in H_2-THF hydrates are occupied by two H_2 molecules and the H_2 occupancy in the large cages could be increased by reducing the concentration of THF, which resulted in a tunable H_2 storage capacity up to 4.0 wt%.(15) By using

View Article Online
DOI: 10.1039/D4CP04820B

ice powders and solid THF in the experiments, Sugahara and co - workers(16) observed a maximum H_2 storage capacity of 3.4 wt%, with the small cages occupied by one H_2 and multiple occupancy of H_2 molecules in the large ones. Nishikawa and co – workers detected H_2 occupancy in large cages of H_2-THF hydrates using *in-situ* Raman spectra without the quenching procedure.(17) On the contrary, it was concluded by other researchers that the small cages in H_2-THF hydrates could only accommodate one H_2 molecule.(18–20) For instance, by using similar experimental procedures as Lee and co – workers,(15) Strobel and co – workers concluded that the storage capacity of H_2 in the H_2-THF hydrates increased with pressure but asymptotically approached 1.0 wt%, with one H_2 in the small cage and the large cages being empty.(20)

To reveal the mechanisms of different occupancy modes of H_2 in the small and large cages, theoretical modeling and molecular dynamic (MD) simulations are conducted to understand the influence of promoters on the storage capacity of H_2. Some research findings support the multiple occupancy of H_2 in the small and large cages by analyzing the variation in energy or hydrate cage volume. For example, Patchkovskii and Tse concluded that the occupancy of two H_2 molecules in the small cages and four H_2 in the large ones favors the stability of the H_2 hydrate structure due to the increased surface contact between H_2 and cage H_2O molecules.(21) Sebastianelli and co – workers also suggested that the strong attractive interaction between H_2 and cage H_2O contributed to the negative ground-state energy when two H_2 molecules occupied the small cage.(22) Alavi and co – workers suggested that the configuration energy did not change significantly with the occupancy modes of H_2 and THF based on classical MD simulation.(23) By using *ab initio* molecular scale simulations, Tachikawa and co - workers concluded that the small and large cages could hold up to 2 and 5 H_2 molecules, respectively.(24) Koh and co – workers revealed that the small cages only needed to expand by around 3% in volume to provide thermodynamically stable

View Article Online
DOI: 10.1039/D4CP04820B

room for two H_2 molecules.(25) On the other hand, some researchers argued against the multiple occupancy of H_2 in the small and large cages.(26) It was suggested that the H_2 molecules are tightly confined in the repulsive potential field with two H_2 molecules occupying the small cages.(27) Liu and co – workers also indicated that the occupancy of two H_2 molecules in the small cage is less favorable and the most stable occupancy mode is the single occupancy of H_2 in the small cage and single H_2 + THF in the large cage.(28) Kang and co – workers concluded that the small cage is occupied by one H_2 molecule, whereas the large cages free of THF could accommodate two to three H_2 molecules.(29)

Despite considerable experimental observations and simulation results, several knowledge gaps associated with the storage capacity of H_2 in H_2-THF hydrates remain. The three key points with respect to the storage capacity of H_2 in the hydrate forms that need to be resolved are: (*i*) feasibility of occupancy of two H_2 molecules in one small hydrate cage; (*ii*) whether the large cages free of THF can be occupied by H_2 when the concentration of THF is lower than the stoichiometric value, i.e., 5.56 mol%; (*iii*) the viability of co-occupancy of THF and H_2 molecule in the same large cages. Also, the influence of hydrogen bonds between THF and cage H_2O molecules on hydrate stability and dynamic motion of H_2 and THF molecules in the small and large cages needs refinement. In this work, the classical MD simulation approach is applied to systematically analyze the abovementioned three factors by combining the dynamic motion of guest and water molecules with the interaction energy, as illustrated in **Figure 1**, which is crucial for the understanding of mechanisms underlying the storage capacity of H_2 in the hydrate form. The cage occupancy modes investigated in this work are based on those either suggested based on previous experimental observations or the ones that are reported viable in simulation work and under realistic conditions. Resolving the knowledge gaps articulated above will unlock the

View Article Online
DOI: 10.1039/D4CP04820B

mechanisms underlying the role of promoters in enabling H_2 storage as hydrates at moderate temperatures and pressures.

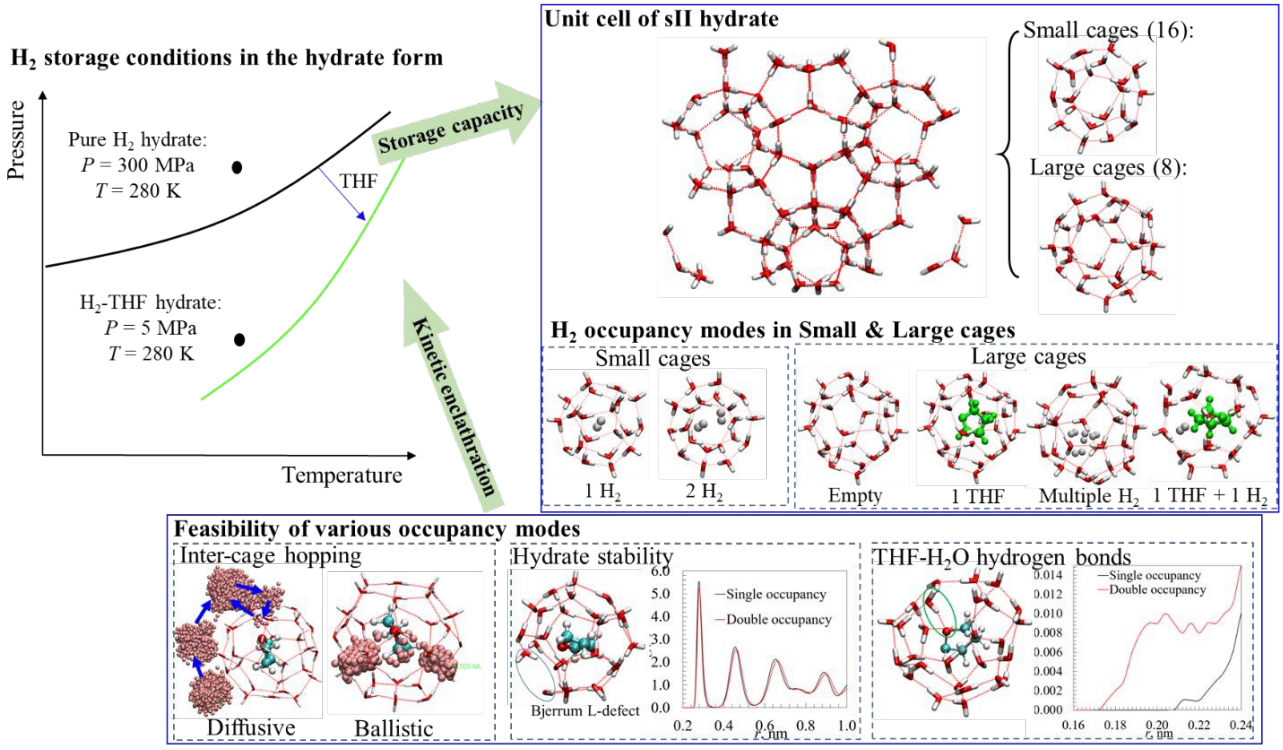

Figure 1. Schematic representation of the approach and methodology used to probe the mechanisms underlying the influence of THF on H_2 hydrate formation.

2. Methodology

Eight different configurations of binary H_2-THF hydrates with various occupancy modes of small and large cages are investigated in this work using MD simulations, as listed in **Table 1**. The occupancy modes of H_2 and THF in each configuration have been reported by either experiments or simulations. *HS1-THF8* configuration denotes that each of the 16 small cages in a unit cell of sII hydrates is occupied by one H_2 molecule, whereas all the 8 large cages are occupied by THF molecules.(9,18–20) *HS2-THF8* configuration is composed with 2 H_2 molecules occupying each small cage and all large cages occupied by THF.(15) By comparing these two configurations,

View Article Online
DOI: 10.1039/D4CP04820B

insights into the impact of various occupancy modes in the small cages on the dynamic motion and structural change are obtained. Configuration *HS2-THF7-HL4* represents the occupancy modes reported by Lee and co – workers,(15) with 7 large cages in a unit cell occupied by THF and the other large one occupied by four H_2 molecules. Each of the small cages is occupied by two H_2 molecules. In *HS1-THF7*, each of the small cages accommodates one H_2 molecule and seven of the large cages in a unit cell are occupied by THF, which denotes the observations by Strobel and co – workers that H_2 molecules could not enter the large cages even when the concentration of THF was lower than the stoichiometric value of 5.56 mol%.(20) As reported by Kang and co - workers, the large cages free of THF could be occupied by 2-3 H_2 molecules, which are investigated in Configurations *HS1-THF7-HL2* and *HS1-THF7-HL3*, respectively.(29) *HS1-(THF+HL)8* denotes the occupancy mode suggested by Kaur and Ramachandran, i.e., each small cage accommodates one H_2 molecule and each large cage is co-occupied by one THF and one H_2 molecule.(30) Liu and co - workers reported a same occupancy mode as *HS1-(THF+HL)8*, but at a lower temperature condition of 140 K.(28) To investigate the impact of pressure and temperature conditions, Configuration *HS1-(THF+HL)8-140K* is designed, with the pressure and temperature of 0.1 MPa and 140 K, respectively. The pressure and temperature conditions in other configurations are 12 MPa and 270 K, respectively.

Table 1. Cage occupancy details of H_2 and THF in the small and large cages of a unit sII cell

Configuration *	Cage occupancy		Reference	Summary / Novel findings
	Small cages (16)	Large cages (8)		
HS1-THF8	Each by one H_2	Each by one THF	9, 18-20	No inter-cage hopping of H_2 molecules; Hydrate structure is stable but with low storage capacity
HS2-THF8	Each by two H_2	Each by one THF	15	Active inter-cage hopping of H_2; High probability of hydrogen bond formation between THF and H_2O; Reduced stability of hydrate structure; Slower decay of THF
HS2-THF7-HL4	Each by two H_2	7 by THF, 1 by four H_2	15	

View Article Online
DOI: 10.1039/D4CP04820B

				orientation due to stronger THF-H_2O interactions
HS1-THF7	Each by one H_2	7 by THF, 1 empty	20	Thermodynamic stability of hydrate is enhanced by occupying three H_2 molecules in the THF-free large cages
HS1-THF7-HL2	Each by one H_2	7 by THF, 1 by two H_2	29	
HS1-THF7-HL3	Each by one H_2	7 by THF, 1 by three H_2	29	
HS1-(THF+HL)8	Each by one H_2	All by one THF + one H_2	30	The inter-cage motion of H_2 molecules evolved from ballistic to diffusive regime with co-occupancy of THF and H_2 in large cages
HS1-(THF+HL)8-140K [a]			28	

Note: * HS, HL, and THF stand for H_2 molecules in the small cages, large cages, and occupancy of THF molecules in the large cages, respectively; [a] P = 0.1 MPa, T = 140 K.

The molecular dynamic simulation package of GROMACS 2020.6(31) is used. According to the sensitivity analysis on the size of simulation box, we did not detect a significant change in the pairwise energy between water and H_2 molecules in the large and small cages with the number of unit cells in the simulation box increasing from 2×2×2 to 5×5×5 (see **Figure S1**). Therefore, a simulation box containing 2×2×2 unit cells of sII hydrates is adopted in this work, with dimensions of 3.462×3.462×3.462 nm. The periodic boundary condition is employed in all three directions of the simulation box. The coordinates of O and H atoms of cage H_2O molecules determined by Takeuchi and co – workers(32) are applied in this work as the configuration of hydrate cages. The center of mass of H_2 (or H_2 clusters in the cases of multiple occupancy) and promoter molecules are placed in the center of the hydrate cages. The interaction between guest and water molecules are regulated by the force fields. In this work, the TIP4P/Ice potential function(33) is applied for H_2O molecules, which has been reported reliable in reproducing the phase boundary conditions of gas hydrates.(34) The three-site model developed by Alavi et al. is employed for H_2 molecules.(35) As for THF molecules, the general AMBER force field (GAFF) is adopted, with the partial charges and atom positions optimized.(12) The H_2O, H_2, and THF molecules are regarded as rigid and constrained using the LINCS algorithm in GROMACS. The parameters of the potential functions are summarized in **Table S2** in the *Supplementary Information*.

View Article Online
DOI: 10.1039/D4CP04820B

A typical simulation algorithm includes an energy minimization step performed to the initial simulation configuration, followed by 100 ps NPT ensemble on the optimized configuration to reach equilibrium state, which is further continued for 1.0 ns in the production stage. The Nose-Hoover thermostat and Berendsen barostat are used for the temperature and pressure coupling, respectively. A time step of 0.2 fs is applied in the equilibrium and production stages. The non-bonded interactions, e.g., van der Waals force and electrostatic forces are modeled using 12-6 Lennard-Jones (LJ) and Columbic models, respectively.(36)

3. Results and Discussions

3.1 Simulation validation

To validate the developed MD simulation models in this work, the distribution and average distance of H_2 molecules in the small and large cages of pure H_2 hydrates are compared with those in the literature. In the pure H_2 hydrates, the small cages are occupied by two H_2 and the large ones by four H_2 molecules, with a simulation pressure and temperature of 0.1 MPa and 100 K respectively, which is within the phase boundary conditions.(35) The initial configuration of the pure H_2 hydrates in the simulation box and that at the end of simulation time are illustrated in **Figure S2** in the *Supplementary Information*.

The two-dimensional (2D) density maps of H_2 molecule distribution in the small and large cages of pure H_2 hydrates are shown in **Figure 2**. The number density is truncated at 20 nm^{-2} to highlight the distribution feature of H_2. The distribution of two H_2 molecules in each small cages separated into two regions away from the cage centers, while that for the four H_2 molecules accumulated in four regions, demonstrating a tetrahedral structure in three dimensions (see **Figure S3** in the *Supplementary Information*). With a closer observation of the 3D distribution profile of the four H_2 molecules in **Figure S3**, it is found that the vertices of the tetrahedral structure pointed

View Article Online
DOI: 10.1039/D4CP04820B

to the four hexagonal faces of the large cages, which is consistent with Burnham and co – workers.(37) Also, the average distance between the two H_2 molecules in the small cages was 2.5-2.6 Å and that between the four H_2 molecules in the large cage is 3.0-3.1 Å, consistent with previous studies.(21,27,28,37) Further, the lattice parameter obtained in this work (1.726 nm) is slightly higher than 1.699 nm obtained by Alavi and co – workers(35) at the same cage occupancy mode and simulation pressure-temperature conditions. This higher lattice parameter is a result of a different force field of H_2O, i.e., SPC/E applied by Alavi and co – workers. The H_2 distribution and hydrate cage structure results indicate reliability of the developed simulation model.

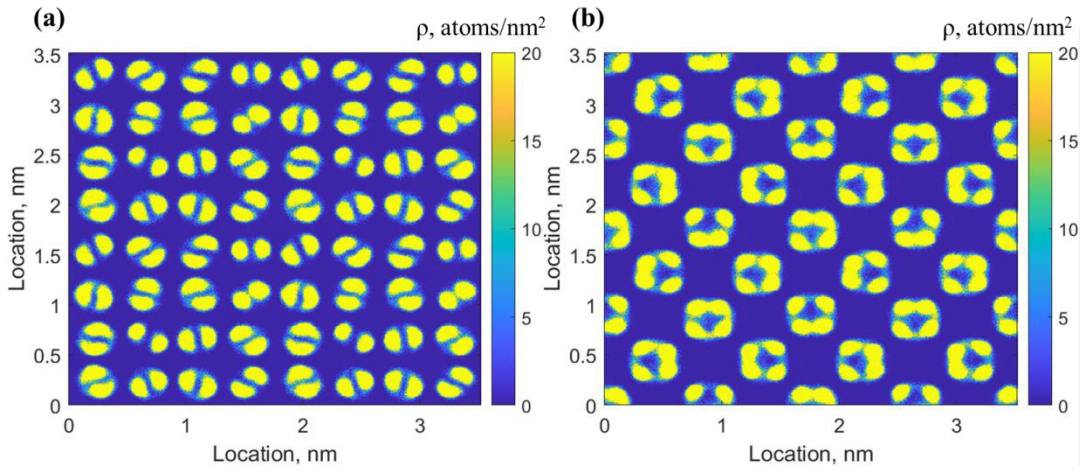

Figure 2. 2D density maps of H_2 molecules distribution in the small (a) and large (b) cages at T = 100 K, P = 0.1 MPa. The density maps are averaged over 1.0 ns of the simulation time.

3.2 Occupancy of two H_2 in small cages

The impact of different occupancy modes of H_2 in the small cages on the dynamic motion and distribution of H_2, THF and cage water molecules, e.g., probability of hydrogen bond formation between THF-oxygen (Ot) and water-hydrogen (Hw), pair-wise interaction energy between different molecules, and stability of hydrate structure is analyzed by comparing the simulation results of various configurations in **Table 1**. It is noted that the impact of H_2 occupancy in small

View Article Online
DOI: 10.1039/D4CP04820B

cages is not significantly influenced by the occupancy modes of H_2 and THF in the large cages. For instance, the findings by comparing results of Configurations *HS1-THF8* and *HS2-THF8* are similar to those by comparing results of Configurations *HS1-THF7-HL3* and *HS2-THF7-HL4*. Therefore, the simulation results of Configurations *HS1-THF8* and *HS2-THF8* are presented as an example to analyze the impact of occupancy mode of H_2 in the small cages.

Impact on dynamic motion of H_2 molecules

Occupancy of two H_2 in the small cages makes the translational motion of H_2 more active, as indicated by the increasing MSD in **Figure 3**. The MSD curve of H_2 molecules showed a steady profile when the small cages were occupied by one H_2 molecule, whereas it increased linearly at an occupancy of two H_2 molecules, with a diffusion constant of 1.7×10^{-8} cm^2/s. This active motion might be attributed to the strong repulsive force between H_2 molecules. The pair-wise potential energy between H_2 was 1.415 kJ/mol with two H_2 molecules occupying the small cages. As a comparison, the interaction between H_2 molecules is attractive when the small cages are occupied by one H_2 molecules, with a pair-wise potential energy between H_2 molecules of -0.075 kJ/mol. The strong repulsive force between H_2 when the small cages are occupied by two H_2 molecules results in the migration of H_2 molecules from cage to cage. This inter-cage hopping is reflected on the 2D density maps of H_2 distribution, as indicated by the non-zero density in the region between cages denoted by the red circles in **Figure 4 (b)**. No inter-cage hopping of H_2 is detected when the small cages are occupied by one H_2 molecule, which is consistent with the observation by Frankcombe et al and Cao et al.(38,39)

View Article Online
DOI: 10.1039/D4CP04820B

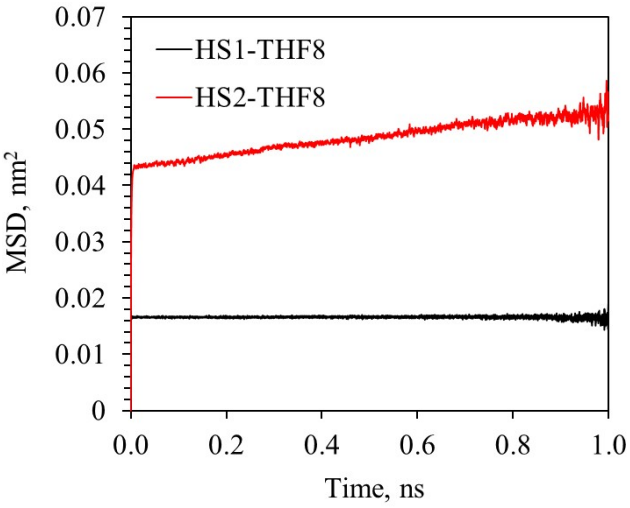

Figure 3. MSD curves of H_2 with small cages occupied by one H_2 (*HS1-THF8*) and two H_2 molecules (*HS2-THF8*).

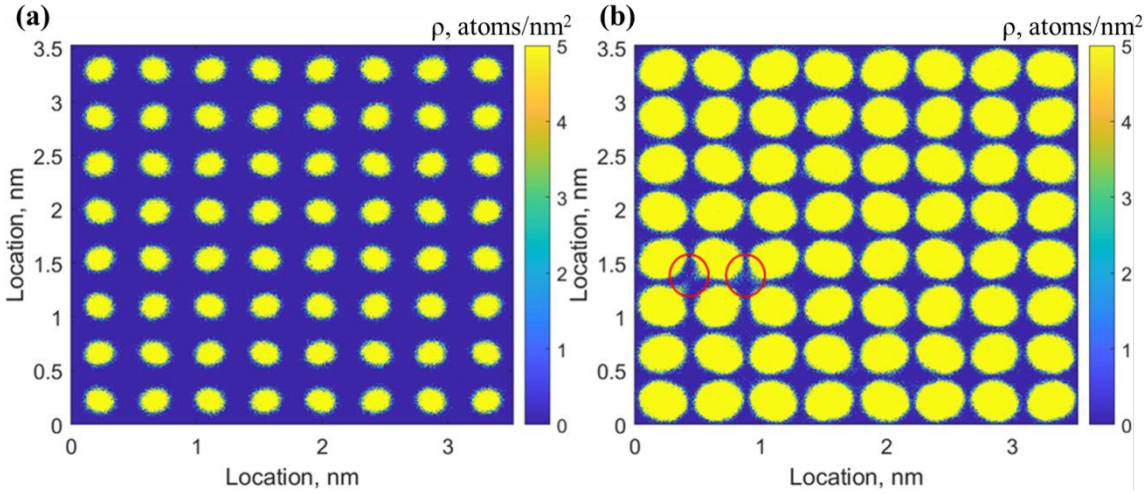

Figure 4. 2D density maps of H_2 distribution in Configurations *HS1-THF8* (a) and *HS2-THF8* (b).

With a closer look into the evolution of the H_2 migration, it is found that the migration may occur to only one of the H_2 molecules occupying a single cage, as shown in **Figure 5**. The **Figures 5 (a1) – 5 (a2)** and **5 (b1) – 5 (b2)** demonstrate the cumulative positions of the first and second H_2 molecules at t = 0 and t = 1.0 ns, respectively. It can be observed that the first H_2 molecule is

View Article Online
DOI: 10.1039/D4CP04820B

retained in the original cage (marked by the green label) throughout the simulation time of 1.0 ns. As for the second H_2 molecule, its inter-cage hopping extended to 4 cages in addition to the original one, with the trajectory described by the blue arrows. It is clearly shown that this H_2 molecule first migrated to a neighboring small cage and the inter-cage hopping from the original small cage to the first cage was through a pentagonal face. Then it continued migrating to two other neighboring small cages through the pentagonal faces. The fourth cage where this H_2 molecule appears is the center large cage which is stably occupied by a THF molecule throughout the simulation time. Two observations are noted in this process: *i*) H_2 migrates from cage to cage and the migration occurs mostly in the small cages; *ii*) H_2 hops into the large cage occupied by the THF molecule through a pentagonal face. For pure H_2 sII hydrates, it is suggested that the energy barrier for the H_2 hopping through a pentagonal face was much higher than a hexagonal one.(24,38,40) However, it is also observed that the H_2 migrated to a neighboring cage through a pentagonal face.(41) The temporary breaking of the hydrogen bonds in the pentagonal faces may facilitate inter-cage hopping of H_2 molecules and some of these hydrogen bonds restored after the migration.(42) Therefore, the observation of H_2 migration through pentagonal faces in Configuration *HS2-THF8* may be attributed to the distorted cage network by the newly formed hydrogen bond between the Ot-Hw in THF and cage water molecules.

View Article Online
DOI: 10.1039/D4CP04820B

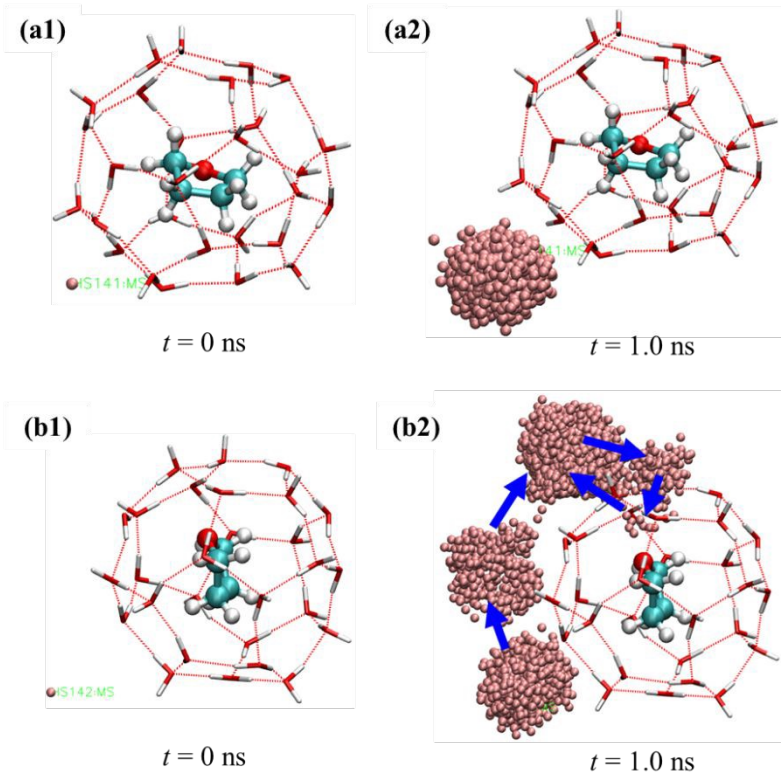

Figure 5. Cumulative positions of the first (a1 and a2) and the second (b1 and b2) H_2 molecule in one small cage of Configuration *HS2-THF8*.

Impact on stability of hydrate structure

The lattice parameter of hydrate cages increases by 1.03% when the number of H_2 molecules occupying the small cages increase from one to two, corresponding to a volume expansion of 3%, which is consistent with the conclusion by Koh and co – workers.(25) Even though an expansion of 3% in the volume of hydrate cages is not pronounced, it has a significant impact on the configuration of hydrate cages, as shown in the RDF curve of oxygen (Ow) pairs of water molecules in **Figure 6 (a)**. It is seen that the peaks become less sharp and shift to a higher radius when the small cages are occupied by two H_2 molecules, indicating a reduced stability of hydrate structure.(36) This reduced stability of hydrate structure may be attributed to the much higher

View Article Online
DOI: 10.1039/D4CP04820B

probability of hydrogen bonds formation between O in THF (Ot) and H in cage H_2O (Hw) molecules when the small cages are occupied by two H_2 molecules, as demonstrated in **Figure 6 (b)**. As suggested by Alavi and co – workers,(43–45) hydrogen bonding between THF and cage water molecules is assumed when the distance of Ot-Hw is shorter than 2.1 Å. The hydrogen bond formed between THF and cage water molecules is marked by the black circle in **Figure 6 (b)**. The formation of hydrogen bond between THF and H_2O is accompanied by the distortion of hydrogen bond network in the hydrate cages, as shown in the blue circle in **Figure 6 (b)**, due to the formation of the Bjerrum L-defect, i.e., the absence of the hydrogen atom between two Ow atoms. It is believed that the guest-cage hydrogen bonds enhance the rotational dynamics of water molecules due to the reduced energy barrier for water rotation in the presence of the Bjerrum L-defect.(46)

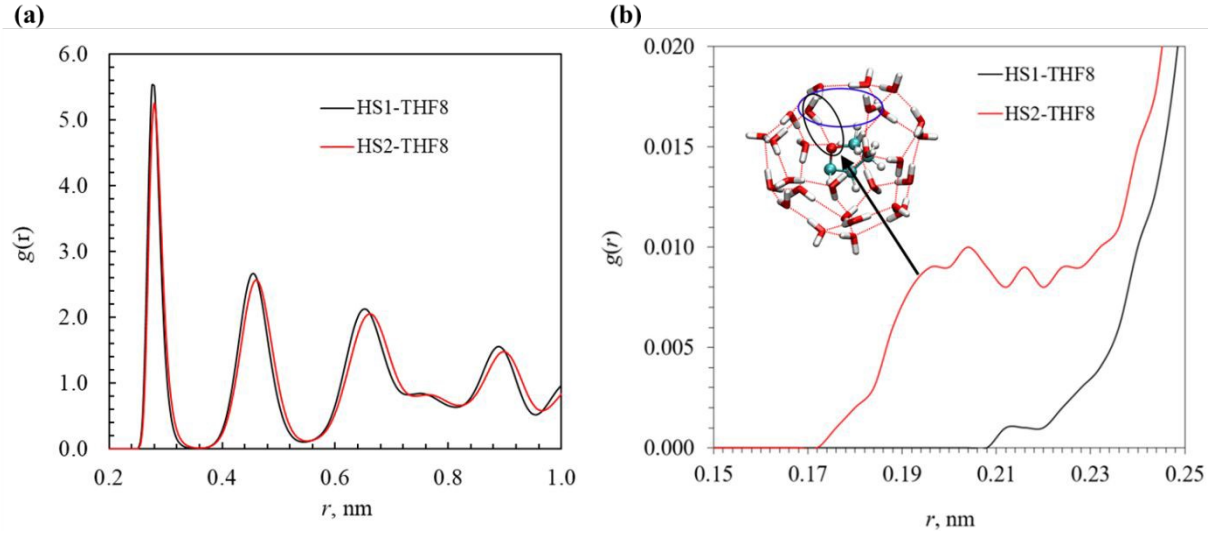

Figure 6. RDF curves of (a) Ow-Ow pairs in H_2O molecules and (b) Ot-Hw pairs in THF and H_2O molecules respectively with different occupancy mode of H_2 in the small cages.

The enlarged volume of hydrate cages by the increased number of H_2 in the hydrate cages also results in slightly more active translational motion of THF. Interestingly, it is found that the decay rate of THF orientation decreases with the increased occupancy of H_2 in the small cages (see

View Article Online
DOI: 10.1039/D4CP04820B

Figure S4 in *Supplementary Information*). Alavi and Ripmeester(47) suggested that the hydrogen bond between THF and cage H_2O molecules slows down the decay of THF orientation, which is consistent with the observation in this work by comparing the probability of hydrogen bond formation as demonstrated in **Figure 6(b)**. The probability of hydrogen bond formation between THF and cage H_2O molecules is greatly elevated when the small cages are occupied by two H_2 molecules, as indicated by the larger area below the RDF curves of O-H pairs around a distance of 0.21 nm. However, this relationship between THF-H_2O hydrogen bonding and the decay of THF orientation is not true when comparing the Configurations *HS1-(THF+HL)8* and *HS1-(THF+HL)8-140K*, which would be further discussed in Section 3.4.

The long-range electrostatic and short-range LJ interactions between water (W), H_2 in the small cages (HS), and THF molecules for in Configurations *HS1-THF8* and *HS2-THF8* is also compared. It is noted that the pair-wise interaction energy (i.e., sum of long-range and short-range interaction energies) is averaged by dividing with the number of molecules for convenient comparison. From the energetics perspective, it is seen that the strongest interaction is between water molecules due to the hydrogen bonding, followed by the interaction between THF and cage water molecules owing to the large size of THF and temporary hydrogen bonds between THF and water molecules. The pair-wise interaction energy between water, H_2, and THF with different occupancy modes in the small cages are compared in **Figure 7**. It is seen that the pair-wise interaction energy of W-HS, HS-THF, and THF-THF are negative due to the overall attractive forces. The absolute value of W-HS and THF-THF interaction energy decreased with the occupancy ratio of H_2 in the small cages due to the expansion of hydrate cages. The absolute value of HS-THF interaction energy is higher because the two H_2 molecules in one small cage are distributed closer to cage edge as shown in **Figure 4 (b)**, which shortened the distance between H_2

View Article Online
DOI: 10.1039/D4CP04820B

and THF. It is noticeable that the interaction energy between the H_2 molecules turned from negative to positive when the occupancy of H_2 in the small cage increased from one to two. As discussed in Section 3.2, this repulsive force between H_2 molecules facilitated the inter-cage hopping of H_2 molecules.

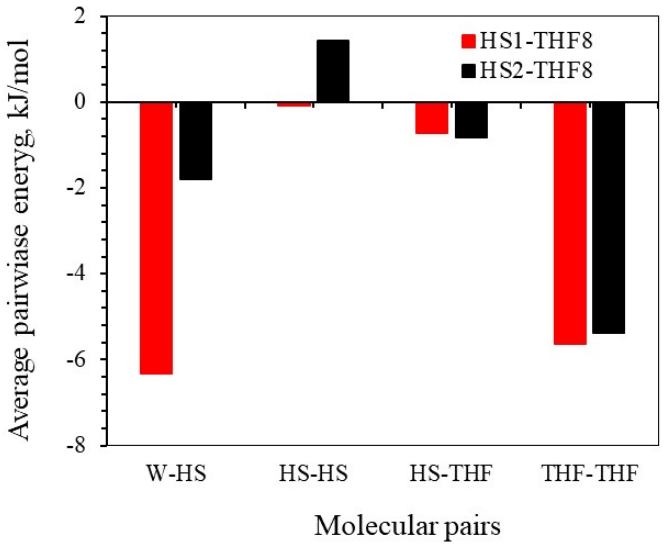

Figure 7. Pair-wise interaction energy between water (W), H_2 in the small cages (HS), and THF in Configurations *HS1-THF8* and *HS2-THF8*.

3.3 Occupancy of H_2 in THF-free large cages

Configurations *HS1-THF7*, *HS1-THF7-HL2*, and *HS1-THF7-HL3* are compared to investigate the impact of H_2 occupancy in the large cage free of THF. It is found that the number of H_2 molecules in the large cage has no noticeable influence on the probability of hydrogen bond formation between THF and cage water molecules. The RDF curves of Ow-Ow pairs in cage H_2O molecules are demonstrated in **Figure 8 (a)**. It is seen that the tetrahedral structure of the water cage is slightly enhanced with more H_2 occupying the THF-free large cages, which is consistent with the slightly less active translational motion of H_2O molecules (see **Figure S5** in

View Article Online
DOI: 10.1039/D4CP04820B

Supplementary Information). Therefore, the occupancy of three H_2 molecules in the THF-free large cages results in slightly more stable hydrate structure. The occupancy modes of H_2 in the THF-free large cages influence the distribution of H_2 molecules, as shown in **Figure 8 (b)**. It is seen that the H_2 molecules became more orderly distributed in the large cages with the number of H_2 molecules increased from two to three. When observing the 2D density maps of H_2 distribution in these two configurations, it is found that the tetrahedral feature of H_2 in the large cages becomes more pronounced when the number of H_2 molecules is increased from two to three, which may suggest that the tetrahedral distribution of H_2 in the large cages is favorable for the stability of hydrate structure.

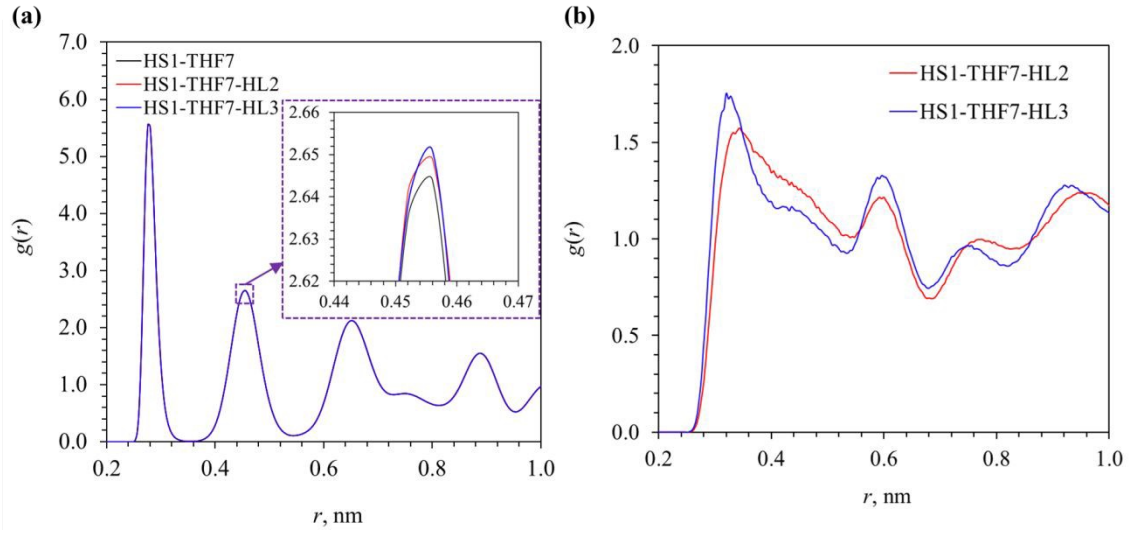

Figure 8. RDF of Ow-Ow pairs in cage H_2O molecules with various occupancy modes of H_2 in the THF-free large cages.

It is interesting to note that even though the occupancy of three H_2 molecules in the THF-free large cages contributes to the thermodynamic stability of hydrate structure, the tunability of H_2 storage in the THF-free large cages is not always captured in the experiments.(20) This observation may be because of the high energy barrier to kinetically enclathrate H_2 molecules into the large

View Article Online
DOI: 10.1039/D4CP04820B

cages. It has been found that the occupancy of H_2 in the THF-free large cages is feasible when ice powders(16) are used to form the H_2-THF hydrates or gas exchange approach is applied to form H_2 hydrates, e.g., enclathrating H_2 into hydrate cages by exchanging with N_2.(48,49) The potential mechanisms for these methods of enhancing the storage capacity of H_2 in the large cages may be due to the reduced energy barrier induced by the pre-existence of cavities in the ice powders and hydrate cages. Therefore, it is important to develop new promoters and techniques to overcome the kinetic barriers for H_2 molecules enclathrating in the promoter-free large cages, which is essential to enhance the storage capacity of hydrate-based hydrogen storage technology.

3.4 Co-occupancy of H_2 and THF in one large cage

It is seen in **Figure 5** that the probability of co-occupancy of H_2 and THF in one large cage is low based on the short time the H_2 molecule is retained in the center large cage, although co-occupancy of THF and small gas molecules, e.g., H_2 and He in the same large cages has been suggested viable according to the ab initio or grand canonical Monte Carlo simulations.(30,50) In this section, Configurations *HS1-(THF+HL)8* and *HS1-(THF+HL)8-140K* are applied to explore the feasibility of co-occupancy of H_2 and THF in one large cage by observing its impact on the dynamic motion of guest and cage water molecules and the hydrate cage stability.

The 2D density maps of H_2 molecules originally occupying the small and large cages are demonstrated in **Figure 9**. By comparing with the typical 2D density maps of one or two H_2 molecules in small cages in **Figure 4**, the 2D density maps of H_2 distribution in **Figure 9 (a)** suggested that some of the small cages are occupied by two H_2 molecules during the simulation. Given that all the small cages are originally occupied by one H_2 molecule, the extra one H_2 molecule migrates from the large cages, which can be confirmed in the 2D density maps of H_2 molecules originated from the large cages in **Figure 9 (b)**. In **Figure 9 (b)**, it is seen that the H_2

View Article Online
DOI: 10.1039/D4CP04820B

molecules originated from the large cages not only showed up in the small cages throughout the simulation time, but also demonstrated bar-like feature in the density map. With a closer observation of one H_2 molecule initially co-occupying a large cage with THF, it turns out this bar-like distribution of the H_2 molecule is a result of the tunneling behavior of H_2 through the hexagonal faces of the large cages, as shown in **Figure 10**. The example in **Figure 10** demonstrates that this H_2 molecule goes back and forth through one hexagonal face in the first 0.7 ns and then moves to another hexagonal face and continues the tunneling behavior to the end of simulation.

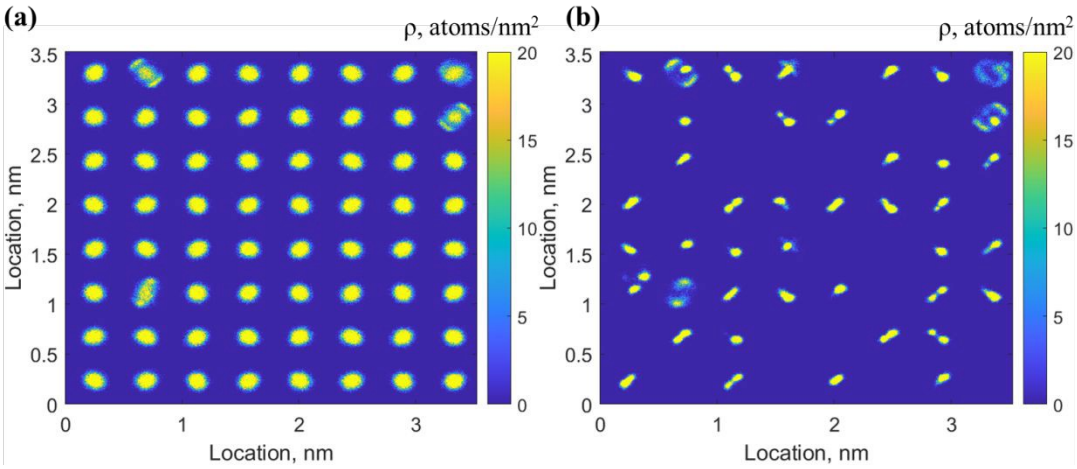

Figure 9. 2D density maps of H_2 distribution originally seated in the small (a) and large (b) cages in Configuration *HS1-(THF+HL)8*.

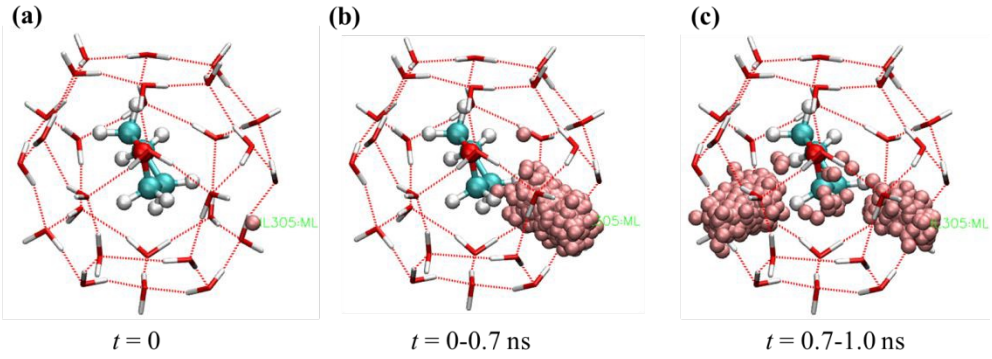

Figure 10. Evolution of the distribution of one H_2 molecule originated from a large cage in Configuration *HS1-(THF+HL)8*.

View Article Online
DOI: 10.1039/D4CP04820B

The impact of pressure and temperature conditions is explored using Configuration *HS1-(THF+HL)8-140K*, where the temperature and pressure are 140 K and 0.1 MPa, respectively. From the RDF curves of Ow-Ow pairs in cage H_2O molecules in **Figure 11**, it is seen that the hydrate cage structure is more stable at P = 0.1 MPa and T = 140 K compared with that at P = 12 MPa and T = 270 K. The peaks in the RDF curve not only became sharper, which indicates more orderly distribution of water molecules in the hydrate cages, they also shifted slightly to left due to the shrinkage of hydrate cages at lower temperature, which is consistent with the smaller lattice parameter (by 1.04%) at the lower temperature conditions.

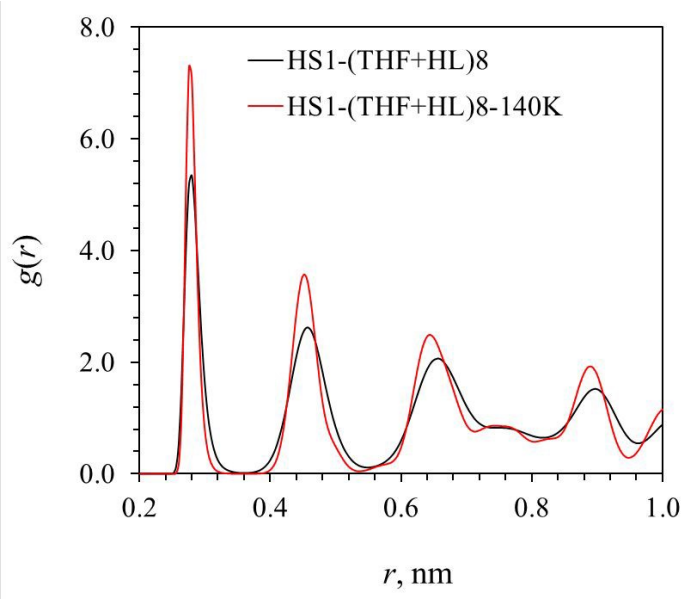

Figure 11. RDF curves of Ow-Ow pairs in cage H_2O molecules with co-occupancy of THF and H_2 in large cages at different pressure-temperature conditions (12 MPa and 270 K for the black curve; 0.1 MPa and 140 K for the red curve).

The impact of the lower temperature and lower pressure condition on the dynamic motion of H_2 molecules initially co-occupying the large cages with THF can be found in **Figure 12**. The MSD curves in **Figure 12 (a)** shows that the motion of H_2 molecules is greatly reduced when the

View Article Online
DOI: 10.1039/D4CP04820B

temperature is decreased to 140 K. However, different from the MSD curves of H_2 in Configuration *HS2-THF8* (see **Figure 3**, where the MSD increased linearly, indicating a diffusive motion), the MSD curves in **Figure 12** suggest a ballistic motion(51,52) of H_2 molecules (MSD $\propto t^2$), which is more pronounced for Configuration *HS1-(THF+HL)8-140K*. By observing the 2D density map of these H_2 molecules in **Figure 12(b)**, it is seen that the migration of H_2 molecules is featured with mostly tunneling behavior, which was also through the hexagonal faces as shown in **Figure S6** in the *Supplementary Information*. Given the fact that the ballistic motion feature is more noticeable in Configuration *HS1-(THF+HL)8-140K* (see **Figure 12 (a)**) and that the tunneling behavior is more remarkable in the migration of these H_2 molecules, it is indicated that the tunneling motion of H_2 molecules originally co-occupying the large cages with THF leads to the ballistic behavior in the MSD curves.

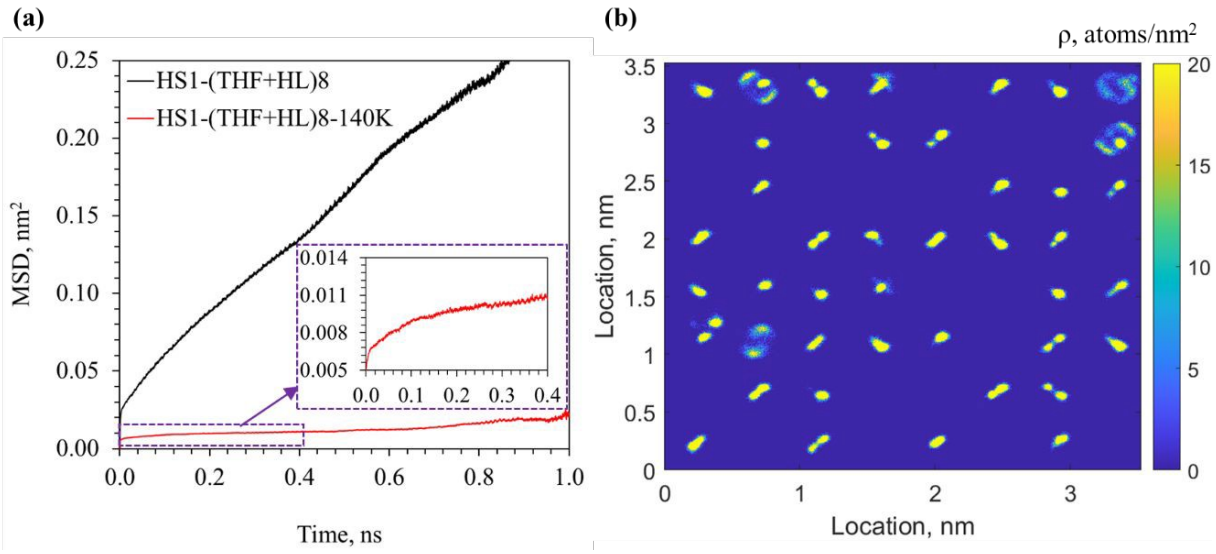

Figure 12. MSD curves of H_2 molecules originally co-occupying the large cages with THF (a) and 2D density map of H_2 distribution in Configuration *HS1-(THF+HL)8-140K* (b).

View Article Online
DOI: 10.1039/D4CP04820B

To further demonstrate the relation between different H_2 inter-cage migration features (i.e., diffusion and tunneling) and features in the MSD curves (i.e., MSD $\propto t$ and MSD $\propto t^2$), the simulation time of Configuration *HS1-(THF+HL)8* is prolonged to 50 ns, with the MSD curves and the 2D density maps of H_2 molecule distribution illustrated in **Figure 13**. It is shown that the MSD $\propto t^2$ relation is captured in the initial stage, ended up with a linear relation. By observing the 2D density maps of H_2 molecules at two different stages, i.e., in the first and last 2 ns, it is found that the probability of tunneling motion of H_2 molecules is greatly reduced in the last 2 ns (See **Figure 13 (b)**), which corresponds to the MSD $\propto t$ feature in the MSD curve. Therefore, it is concluded that the MSD $\propto t^2$ feature in the MSD curve of H_2 molecules results from the tunneling motion of H_2 molecules through the hexagonal faces, whereas the inter-cage hopping of H_2 molecules through diffusion leads to a linear feature in the MSD curves, which also applies to inter-cage hopping of H_2 molecules initially occupying the small cages (e.g., Configuration *HS2-THF8*). Also, the probability of hydrogen bond formation between THF and H_2O molecules is low when the ballistic motion dominates as shown in **Figure 14 (b)**, which means that the hydrate structure is less likely distorted in the ballistic regime. In contrast, when the hydrate structure is less stable, the ballistic motion of H_2 molecules in the initial stage will be gradually replaced by the diffusive motion. These results may indicate that the stable co-occupancy of H_2 and THF in one large cage is possible, accompanied by the ballistic motion of H_2 molecules. In other words, the ballistic motion is favorable for a higher storage capacity of hydrogen in the hydrate form, due to the possible co-occupancy of H_2 and THF in one hydrate cage. However, it requires a more stable hydrate structure, i.e., at higher pressure or lower temperature conditions.

View Article Online
DOI: 10.1039/D4CP04820B

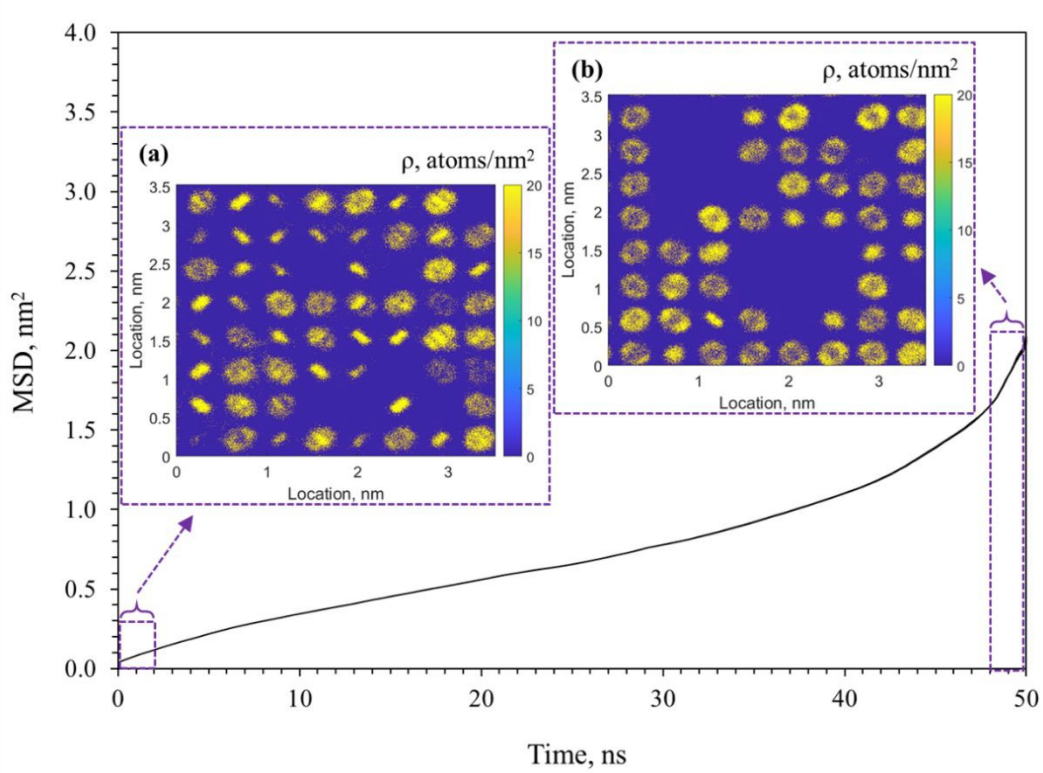

Figure 13. MSD curve of H_2 molecules originally co-occupying the large cages with THF and 2D density maps of H_2 distribution in the first 2 ns (a) and last 2 ns (b) with the simulation time of Configuration *HS1-(THF+HL)8* prolonged to 50 ns.

The impact of temperature and pressure on the decay rate of THF orientation is demonstrated in **Figure 14 (a)**. It is seen that the decay rate is significantly reduced in Configuration *HS1-(THF+HL)8-140K*. As discussed in Section 3.2, it is suggested that the slower decay of THF orientation in H_2-THF hydrates is due to the higher probability of hydrogen bond formation between THF and cage water molecules.(42) However, it is observed in **Figure 14 (b)** that the probability of hydrogen bond formation in Configuration *HS1-(THF+HL)8-140K* is greatly reduced. Therefore, the relationship between stronger hydrogen bonds of THF-H_2O and smaller decay rate of THF orientation is not valid. To explore the cause of slower decay of THF orientation,

View Article Online
DOI: 10.1039/D4CP04820B

the pair-wise interaction energy between THF and cage water molecules in different configurations is compared. It is found that the decay rate of THF orientation is regulated by the interaction energy between THF and H_2O molecules in general. For instance, the pair-wise interaction energy of THF-H_2O is -54.95 kJ/mol and -57.52 kJ/mol respectively for Configurations *HS1-(THF+HL)8* and *HS1-(THF+HL)8-140K*. The higher interaction force between THF and H_2O arises from the the short-range LJ interaction, which may be attributed to the shorter distance between THF and H_2O with the shrunk cages. Another example is that the pair-wise interaction energy of THF-H_2O for Configurations *HS1-THF8* and *HS2-THF8* is -55.45 kJ/mol and -56.37 kJ/mol, respectively. This stronger interaction between THF and H_2O results in slower decay of THF orientation (see **Figure S4**).

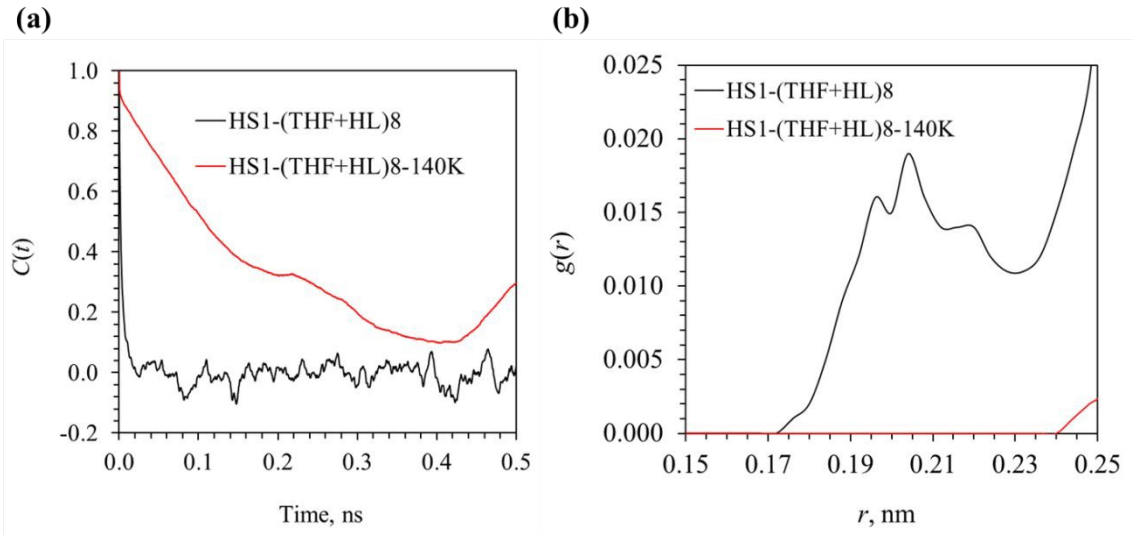

Figure 14. RACF curve of THF (a) and RDF of O-H pairs in THF and H_2O molecules (b).

4. Conclusions

The influence of different occupancy modes of H_2 in the small and large cages on the dynamic motion of gas and water molecules and hydrate structure stability to inform the storage capacity of H_2 in H_2-THF hydrate, is elucidated using classical molecular dynamics (MD) simulations.

View Article Online
DOI: 10.1039/D4CP04820B

Eight configurations with occupancy modes determined or suggested by previous experiments and simulation research are used to investigate the impact of (*i*) occupancy of two H_2 molecules in the small cages, (*ii*) occupancy of H_2 molecules in the THF-free large cages, and (*iii*) co-occupancy of H_2 and THF in one large cage. The following conclusions are drawn based on the configurations designed to address key knowledge gaps in hydrogen storage as hydrates:

(1) Occupancy of two H_2 molecules in small cages: The presence of two H_2 molecules in the small cages induced strong repulsive forces between the two H_2 molecules within a confined space, leading to active inter-cage hopping. The inter-cage migration occurred predominantly among small cages via pentagonal faces, with occasional migration into THF-occupied large cages. This phenomenon indicates that the distortion of the hydrate framework due to THF-water hydrogen bonding reduces the energy barrier for H_2 migration through pentagonal faces. Structurally, the occupancy of two H_2 molecules caused a 1.03% increase in lattice parameter, corresponding to a 3% expansion in cage volume. This expansion weakened the stability of the hydrate framework, as reflected by broader RDF peaks and disrupted hydrogen bonding among water molecules.

(2) Occupancy of H_2 molecules in THF-Free large cages: The occupancy of two or three H_2 molecules in large cages free of THF resulted in enhanced tetrahedral arrangements of H_2 molecules, particularly when three H_2 molecules were present. The tetrahedral distribution is energetically favorable and contributes to slightly improved hydrate stability. The findings suggest that higher occupancy in THF-free large cages can stabilize the hydrate framework, albeit the experimental realization of such configurations may face kinetic challenges. Approaches such as using ice powders or gas exchange methods could overcome these barriers by reducing the energy required for enclathration.

View Article Online
DOI: 10.1039/D4CP04820B

(3) Co-occupancy of H_2 and THF in large cages: The inter-cage migration of H_2 molecules when co-occupying large cages with THF demonstrated two motion features, i.e., ballistic motion (MSD $\propto t^2$) due to the tunneling behavior in the initial stage and diffusive motion (MSD $\propto t$) in the late stage. Prolonged simulations confirmed that the ballistic regime is associated with greater hydrate stability due to reduced hydrogen bond distortion. The probability of hydrogen bond formation between THF and H_2O is low when the tunneling migration of H_2 molecules is dominant in the inter-cage hopping, which may indicate that the tunneling migration behavior is enabled by a more stable hydrate structure, and is more favorable for achieving a higher storage capacity of H_2 hydrates due to the co-occupancy mode. The decay rate of THF orientation is regulated by the interaction energy between THF and cage water molecules. A stronger interaction between THF and H_2O molecules leads to slower decay of THF orientation.

By systematically analyzing the dynamic motion of H_2 and THF molecules and their interactions with the hydrate framework, this study bridges longstanding knowledge gaps in understanding hydrogen storage capacity and hydrate stability. The insights into the effects of occupancy modes on molecular dynamics and structural integrity provide valuable guidance for optimizing hydrate-based hydrogen storage systems under moderate temperature and pressure conditions, paving the way for advancing sustainable hydrogen storage solutions that align with the goals of a sustainable energy future.

Author contributions

Ruyi Zheng: writing – original draft, concept, data curation, formal analysis, investigation, methodology, validation; Sohaib Mohammed: writing – review & editing, formal analysis, methodology, validation; Yang Jia: writing – editing, validation; Rituparna Hazra: writing –

View Article Online
DOI: 10.1039/D4CP04820B

review & editing, methodology; Greeshma Gadikota: writing – concept, review & editing, supervision, conceptualization, resources, formal analysis.

Conflicts of interest

G. G. is the co-founder of Carbon To Stone, a company focused on commercializing technologies for industrial carbon management.

Acknowledgements

This work was supported as part of the Multi-Scale Fluid-Solid Interactions in Architected and Natural Materials (MUSE), an Energy Frontier Research Center funded by the U.S. Department of Energy, Office of Science, Basic Energy Sciences under Award # DE-SC0019285.

References

1. Gupta A, Baron GV, Perreault P, Lenaerts S, Ciocarlan RG, Cool P, Mileo PG, Rogge S, Van Speybroeck V, Watson G, Van der Voort P. Hydrogen clathrates: Next generation hydrogen storage materials. Energy Storage Materials. 2021 Oct 1;41:69-107.
2. Zheng R, Germann TC, Huang L, Mehana M. Driving mechanisms of quartz wettability alteration under in-situ H2 geo-storage conditions: Role of organic ligands and surface morphology. International Journal of Hydrogen Energy. 2024 Mar 15;59:1388-98.
3. Zheng R, Germann TC, Gross M, Mehana M. Molecular insights into the impact of surface chemistry and pressure on quartz wettability: resolving discrepancies for hydrogen geo-storage. ACS Sustainable Chemistry & Engineering. 2024 Mar 26;12(14):5555-63.
4. Heinemann N, Alcalde J, Miocic JM, Hangx SJ, Kallmeyer J, Ostertag-Henning C, Hassanpouryouzband A, Thaysen EM, Strobel GJ, Schmidt-Hattenberger C, Edlmann K. Enabling large-scale hydrogen storage in porous media–the scientific challenges. Energy & Environmental Science. 2021;14(2):853-64.

View Article Online
DOI: 10.1039/D4CP04820B

5. Zheng R, Germann TC, Gross M, Mehana M. Hydrogen diffusion in slit pores: Role of temperature, pressure, confinement, and roughness. Energy & Fuels. 2024 Oct 23;38(21):21642-50.
6. Struzhkin VV, Militzer B, Mao WL, Mao HK, Hemley RJ. Hydrogen storage in molecular clathrates. Chemical Reviews. 2007 Oct 10;107(10):4133-51.
7. Zhang Y, Bhattacharjee G, Kumar R, Linga P. Solidified hydrogen storage (Solid-HyStore) via clathrate hydrates. Chemical Engineering Journal. 2022 Mar 1;431:133702.
8. Zheng R, Wang Z, Li X, Fan Z, Negahban S. Structural and dynamic analyses of CH_4 - C_2H_6 - CO_2 hydrates using thermodynamic modeling and molecular dynamic simulation. The Journal of Chemical Thermodynamics. 2022 Jun 1;169:106749.
9. Florusse LJ, Peters CJ, Schoonman J, Hester KC, Koh CA, Dec SF, Marsh KN, Sloan ED. Stable low-pressure hydrogen clusters stored in a binary clathrate hydrate. Science. 2004 Oct 15;306(5695):469-71.
10. Mao WL, Mao HK, Goncharov AF, Struzhkin VV, Guo Q, Hu J, Shu J, Hemley RJ, Somayazulu M, Zhao Y. Hydrogen clusters in clathrate hydrate. Science. 2002 Sep 27;297(5590):2247-9.
11. Mao WL, Mao HK. Hydrogen storage in molecular compounds. Proceedings of the National Academy of Sciences. 2004 Jan 20;101(3):708-10.
12. Atamas AA, Cuppen HM, Koudriachova MV, de Leeuw SW. Monte Carlo calculations of the free energy of binary sII hydrogen clathrate hydrates for identifying efficient promoter molecules. The Journal of Physical Chemistry B. 2013 Jan 31;117(4):1155-65.
13. Lal B, Nashed O. Chemical additives for gas hydrates. Springer Nature; 2019 Oct 1.

View Article Online
DOI: 10.1039/D4CP04820B

14. Veluswamy HP, Kumar R, Linga P. Hydrogen storage in clathrate hydrates: Current state of the art and future directions. Applied Energy. 2014 Jun 1;122:112-32.
15. Lee H, Lee JW, Kim DY, Park J, Seo YT, Zeng H, Moudrakovski IL, Ratcliffe CI, Ripmeester JA. Tuning clathrate hydrates for hydrogen storage. Nature. 2005 Apr 7;434(7034):743-6.
16. Sugahara T, Haag JC, Prasad PS, Warntjes AA, Sloan ED, Sum AK, Koh CA. Increasing hydrogen storage capacity using tetrahydrofuran. Journal of the American Chemical Society. 2009 Oct 21;131(41):14616-7.
17. Nishikawa A, Tanabe T, Kitamura K, Matsumoto Y, Ohgaki K, Sugahara T. In situ Raman spectra of hydrogen in large cages of hydrogen+ tetrahydrofuran mixed hydrates. Chemical Engineering Science. 2013 Sep 20;101:1-4.
18. Hashimoto S, Murayama S, Sugahara T, Sato H, Ohgaki K. Thermodynamic and Raman spectroscopic studies on H_2 + tetrahydrofuran + water and H_2 + tetra-n-butyl ammonium bromide + water mixtures containing gas hydrates. Chemical Engineering Science. 2006 Dec 1;61(24):7884-8.
19. Hester KC, Strobel TA, Sloan ED, Koh CA, Huq A, Schultz AJ. Molecular hydrogen occupancy in binary THF − H_2 clathrate hydrates by high resolution neutron diffraction. The Journal of Physical Chemistry B. 2006 Jul 27;110(29):14024-7.
20. Strobel TA, Taylor CJ, Hester KC, Dec SF, Koh CA, Miller KT, Sloan ED. Molecular hydrogen storage in binary THF − H_2 clathrate hydrates. The Journal of Physical Chemistry B. 2006 Aug 31;110(34):17121-5.
21. Patchkovskii S, Tse JS. Thermodynamic stability of hydrogen clathrates. Proceedings of the National Academy of Sciences. 2003 Dec 9;100(25):14645-50.

View Article Online
DOI: 10.1039/D4CP04820B

22. Sebastianelli F, Xu M, Elmatad YS, Moskowitz JW, Bačić Z. Hydrogen molecules in the small dodecahedral cage of a clathrate hydrate: quantum translation − rotation dynamics of the confined molecules. The Journal of Physical Chemistry C. 2007 Feb 15;111(6):2497-504.
23. Alavi S, Ripmeester JA, Klug DD. Molecular-dynamics simulations of binary structure II hydrogen and tetrahydrofurane clathrates. The Journal of Chemical Physics. 2006 Jan 7;124(1).
24. Tachikawa H, Iyama T, Kawabata H. Maximum capacity of the hydrogen storage in water clusters. Physics and Chemistry of Liquids. 2009 Feb 1;47(1):103-9.
25. Koh DY, Kang H, Jeon J, Ahn YH, Park Y, Kim H, Lee H. Tuning cage dimension in clathrate hydrates for hydrogen multiple occupancy. The Journal of Physical Chemistry C. 2014 Feb 13;118(6):3324-30.
26. Krishnan Y, Ghaani MR, Desmedt A, English NJ. Hydrogen inter-cage hopping and cage occupancies inside hydrogen hydrate: Molecular-dynamics analysis. Applied Sciences. 2020 Dec 30;11(1):282.
27. Wang J, Lu H, Ripmeester JA, Becker U. Molecular-dynamics and first-principles calculations of raman spectra and molecular and electronic structure of hydrogen clusters in hydrogen clathrate hydrate. The Journal of Physical Chemistry C. 2010 Dec 16;114(49):21042-50.
28. Liu J, Hou J, Xu J, Liu H, Chen G, Zhang J. Ab initio study of the molecular hydrogen occupancy in pure H_2 and binary H_2 - THF clathrate hydrates. International journal of hydrogen energy. 2017 Jul 6;42(27):17136-43.
29. Kang DW, Lee W, Ahn YH, Lee JW. Exploring tuning phenomena of THF-H2 hydrates via molecular dynamics simulations. Journal of Molecular Liquids. 2022 Mar 1;349:118490.
30. Kaur SP, Ramachandran CN. Hydrogen-tetrahydrofuran mixed hydrates: A computational study. International Journal of Hydrogen Energy. 2018 Oct 18;43(42):19559-66.

View Article Online
DOI: 10.1039/D4CP04820B

31. Abraham MJ, Murtola T, Schulz R, Páll S, Smith JC, Hess B, Lindahl E. GROMACS: High performance molecular simulations through multi-level parallelism from laptops to supercomputers. SoftwareX. 2015 Sep 1;1:19-25.
32. Takeuchi F, Hiratsuka M, Ohmura R, Alavi S, Sum AK, Yasuoka K. Water proton configurations in structures I, II, and H clathrate hydrate unit cells. The Journal of Chemical Physics. 2013 Mar 28;138(12).
33. Abascal JL, Sanz E, García Fernández R, Vega C. A potential model for the study of ices and amorphous water: TIP4P/Ice. The Journal of Chemical Physics. 2005 Jun 15;122(23).
34. Conde MM, Vega C. Determining the three-phase coexistence line in methane hydrates using computer simulations. The Journal of Chemical Physics. 2010 Aug 14;133(6).
35. Alavi S, Ripmeester JA, Klug DD. Molecular-dynamics study of structure II hydrogen clathrates. The Journal of Chemical Physics. 2005 Jul 8;123(2).
36. Zheng R, Li X, Negahban S. Molecular-level insights into the structure stability of CH4-C2H6 hydrates. Chemical Engineering Science. 2022 Jan 16;247:117039.
37. Burnham CJ, Futera Z, English NJ. Quantum and classical inter-cage hopping of hydrogen molecules in clathrate hydrate: Temperature and cage-occupation effects. Physical Chemistry Chemical Physics. 2017;19(1):717-28.
38. Frankcombe TJ, Kroes GJ. Molecular dynamics simulations of type-sII hydrogen clathrate hydrate close to equilibrium conditions. The Journal of Physical Chemistry C. 2007 Sep 6;111(35):13044-52.
39. Cao H, English NJ, MacElroy JM. Diffusive hydrogen inter-cage migration in hydrogen and hydrogen-tetrahydrofuran clathrate hydrates. The Journal of Chemical Physics. 2013 Mar 7;138(9).

View Article Online
DOI: 10.1039/D4CP04820B

40. Alavi S, Ripmeester J. Hydrogen-gas migration through clathrate hydrate cages. Angewandte Chemie International Edition. 2007 Aug 13;46(32):6102.
41. Willow SY, Xantheas SS. Enhancement of hydrogen storage capacity in hydrate lattices. Chemical Physics Letters. 2012 Feb 16;525:13-8.
42. Gorman PD, English NJ, MacElroy JM. Dynamical cage behaviour and hydrogen migration in hydrogen and hydrogen-tetrahydrofuran clathrate hydrates. The Journal of Chemical Physics. 2012 Jan 28;136(4).
43. Alavi S, Susilo R, Ripmeester JA. Linking microscopic guest properties to macroscopic observables in clathrate hydrates: Guest-host hydrogen bonding. The Journal of Chemical Physics. 2009 May 7;130(17).
44. Alavi S, Udachin K, Ripmeester JA. Effect of guest–host hydrogen bonding on the structures and properties of clathrate hydrates. Chemistry–A European Journal. 2010 Jan 18;16(3):1017-25.
45. Alavi S, Shin K, Ripmeester JA. Molecular dynamics simulations of hydrogen bonding in clathrate hydrates with ammonia and methanol guest molecules. Journal of Chemical & Engineering Data. 2015 Feb 12;60(2):389-97.
46. Alavi S, Ripmeester JA. Molecular simulations of clathrate hydrates. Clathrate Hydrates: Molecular Science and Characterization. 2022 Apr 11;2:283-367.
47. Alavi S, Ripmeester JA. Effect of small cage guests on hydrogen bonding of tetrahydrofuran in binary structure II clathrate hydrates. The Journal of Chemical Physics. 2012 Aug 7;137(5).
48. Lu H, Wang J, Liu C, Ratcliffe CI, Becker U, Kumar R, Ripmeester J. Multiple H_2 occupancy of cages of clathrate hydrate under mild conditions. Journal of the American Chemical Society. 2012 Jun 6;134(22):9160-2.

View Article Online
DOI: 10.1039/D4CP04820B

49. Park S, Koh DY, Kang H, Lee JW, Lee H. Effect of molecular nitrogen on multiple hydrogen occupancy in clathrate hydrates. The Journal of Physical Chemistry C. 2014 Sep 4;118(35):20203-8.

50. Papadimitriou NI, Tsimpanogiannis IN, Stubos AK, Martin A, Rovetto LJ, Peters CJ. Unexpected behavior of helium as guest gas in sII binary hydrates. The Journal of Physical Chemistry Letters. 2010 Mar 18;1(6):1014-7.

51. Han S, Choi MY, Kumar P, Stanley HE. Phase transitions in confined water nanofilms. Nature Physics. 2010 Sep;6(9):685-9.

52. Mohammed S, Asgar H, Benmore CJ, Gadikota G. Structure of ice confined in silica nanopores. Physical Chemistry Chemical Physics. 2021;23(22):12706-17.

View Article Online
DOI: 10.1039/D4CP04820B

Data Availability Statement

The data supporting this article have been included in the main manuscript and as part of the Supplementary Information.